Essential role of peripheral node addressin in lymphocyte homing to nasal-associated lymphoid tissues and allergic immune responses

Yukari Ohmichi,[1] Jotaro Hirakawa,[1] Yasuyuki Imai,[1] Minoru Fukuda,[2] and Hiroto Kawashima[1,3]

[1]Laboratory of Microbiology and Immunology and the Global Center of Excellence Program, School of Pharmaceutical Sciences, University of Shizuoka, Shizuoka 422-8526, Japan
[2]Glycobiology Unit, Sanford-Burnham Medical Research Institute, La Jolla, CA 92037
[3]PRESTO, Japan Science and Technology Agency, Kawaguchi 332-0012, Japan

Nasal-associated lymphoid tissue (NALT) is a mucosal immune tissue that provides immune responses against inhaled antigens. Lymphocyte homing to NALT is mediated by specific interactions between lymphocytes and high endothelial venules (HEVs) in NALT. In contrast to HEVs in other mucosal lymphoid tissues, NALT HEVs strongly express peripheral node addressins (PNAds) that bear sulfated glycans recognized by the monoclonal antibody MECA-79. We investigated the role of PNAd in lymphocyte homing to NALT using sulfotransferase *N*-acetylglucosamine-6-*O*-sulfotransferase (GlcNAc6ST) 1 and GlcNAc6ST-2 double knockout (DKO) mice. The expression of PNAd in NALT HEVs was eliminated in DKO mice. Short-term homing assays indicated that lymphocyte homing to NALT was diminished by 90% in DKO mice. Production of antigen-specific IgE and the number of sneezes in response to nasally administered ovalbumin were also substantially diminished. Consistently, the NALT of DKO mice showed reduced production of IL-4 and increased production of IL-10 together with an increase in $CD4^+CD25^+$ regulatory T cells (T_{reg} cells). Compared with the homing of $CD4^+CD25^-$ conventional T cells, the homing of $CD4^+CD25^+$ T_{reg} cells to NALT was less dependent on the L-selectin–PNAd interaction but was partially dependent on PSGL-1 (P-selectin glycoprotein ligand 1) and CD44. These results demonstrate that PNAd is essential for lymphocyte homing to NALT and nasal allergic responses.

CORRESPONDENCE
Hiroto Kawashima:
kawashih@u-shizuoka-ken.ac.jp

Abbreviations used: APC, allophycocyanin; CLN, cervical LN; CT, cholera toxin; DKO, GlcNAc6ST-1 and GlcNAc6ST-2 double KO; GlcNAc6ST, *N*-acetylglucosamine-6-*O*-sulfotransferase; HA, hyaluronic acid; HEV, high endothelial venule; MAdCAM-1, mucosal addressin cell adhesion molecule 1; MALT, mucosa-associated lymphoid tissue; MLN, mesenteric LN; NALT, nasal-associated lymphoid tissue; PLN, peripheral LN; PNAd, peripheral node addressin; PP, Peyer's patch; PSGL-1, P-selectin glycoprotein ligand 1; T_{conv} cell, conventional T cell; T_{reg} cell, regulatory T cell.

Lymphocytes migrate into the parenchyma of secondary lymphoid organs, such as peripheral LNs (PLNs) and Peyer's patches (PPs), through specialized blood vessels called high endothelial venules (HEVs; Butcher and Picker, 1996; von Andrian and Mempel, 2003). This process is important for the immune system to efficiently recognize antigens accumulated in the secondary lymphoid organs. HEVs have a characteristic cuboidal morphology and a prominent Golgi complex where unique sulfated glycans are synthesized (Girard and Springer, 1995). Lymphocyte migration is achieved by a series of interactions between lymphocytes and HEVs (Springer, 1994): (1) lymphocyte rolling mediated by L-selectin on the lymphocytes and sulfated glycans on the HEVs; (2) activation of lymphocytes by chemokines presented on the surface of HEVs by heparan sulfate; (3) firm attachment of lymphocytes mediated by integrins; and (4) transmigration.

Studies of the carbohydrate-based ligands for L-selectin expressed on LN HEVs have identified several sialomucins, including GlyCAM-1, CD34, podocalyxin-like protein, and Sgp200 (Rosen, 2004), that are reactive with the MECA-79 antibody (Streeter et al., 1988), which blocks L-selectin–mediated lymphocyte binding to HEVs. Peripheral node addressin (PNAd) is the general term for MECA-79–reactive antigens. The binding of these sialomucins to L-selectin is dependent on their decoration with a specific carbohydrate structure known as 6-sulfo sialyl Lewis X (Sialic acidα2-3Galβ1-4[Fucα1-3(sulfo-6)]GlcNAcβ1-R; Rosen, 2004; Kawashima, 2006). The 6-sulfo

Y. Ohmichi and J. Hirakawa contributed equally to this paper.

The Rockefeller University Press $30.00
J. Exp. Med. Vol. 208 No. 5 1015-1025
www.jem.org/cgi/doi/10.1084/jem.20101786

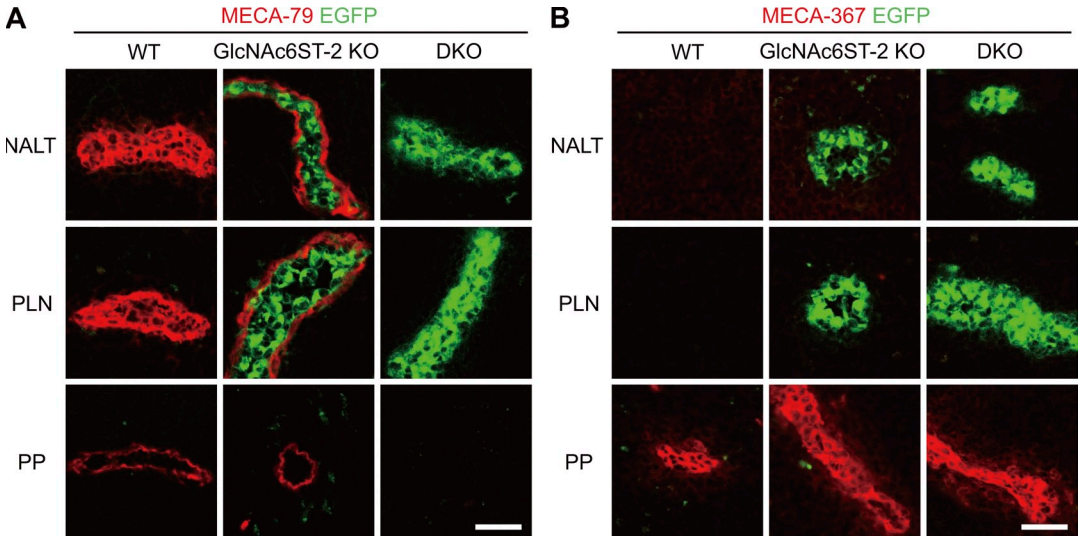

Figure 1. Expression of the chimeric protein GlcNAc6ST-2-EGFP, MECA-79, and MECA-367 antigens. Frozen sections of NALT, PLNs, and PPs from WT, GlcNAc6ST-2–deficient (GlcNAc6ST-2 KO), and GlcNAc6ST-1 and GlcNAc6ST-2 DKO mice were stained with MECA-79 (A, red) or MECA-367 (B, red) mAb. Green fluorescence is from the GlcNAc6ST-2–EGFP chimeric protein that had been knocked-in to the GlcNAc6ST-2 locus (Hiraoka et al., 2004; Kawashima et al., 2005). Bars, 30 µm. Data are representative of four independent experiments.

sialyl Lewis X structure is present in either the core 2 or extended core 1 branch (or both) of L-selectin ligand *O*-glycans. MECA-79 antibody recognizes *O*-glycans containing 6-sulfo *N*-acetylglucosamine in the extended core 1 structure (Yeh et al., 2001). It has been reported that *N*-glycans modified with the 6-sulfo sialyl Lewis X structure are also important for lymphocyte homing to PLNs (Mitoma et al., 2007).

To determine the sulfation requirement of L-selectin ligands in vivo, mice deficient in two HEV-expressed sulfotransferases, *N*-acetylglucosamine-6-*O*-sulfotransferase (GlcNAc6ST) 1 and GlcNAc6ST-2 (also called HEC-GlcNAc6ST or L-selectin ligand sulfotransferase) were generated (Kawashima et al., 2005; Uchimura et al., 2005). Immunofluorescence studies revealed that binding of the MECA-79 antibody to LN HEVs of the GlcNAc6ST-1 and GlcNAc6ST-2 double KO (DKO) mice was completely abrogated, indicating that GlcNAc-6-*O*-sulfation in the extended core 1 branch of *O*-glycans in HEVs was absent in DKO mice. Accordingly, DKO mice showed a significant reduction in lymphocyte homing to PLNs. Contact hypersensitivity responses were also significantly diminished in DKO mice as the result of a reduction in lymphocyte trafficking to the draining LNs (Kawashima et al., 2005).

Nasal-associated lymphoid tissue (NALT) is a mucosal lymphoid tissue in rodents that is considered to be equivalent to Waldeyer's ring in humans, including tonsils and adenoids (Hellings et al., 2000). More recent studies examined human nasal tissue blocks of 150 children who had died in the first 2 yr of life and indicated the presence of a NALT-like structure in humans as a morphologically distinct structure from tonsils and adenoids disseminated in the nasal mucosa, with morphological features typical of secondary lymphoid organs, such as HEVs and lymphoid follicles, sometimes with germinal centers (Debertin et al., 2003). Studies using rodents have revealed that PPs and NALT are two of the main components of mucosa-associated lymphoid tissue (MALT) and are important inductive sites for mucosal immunity against antigens entering through the mucus by ingestion and inhalation, respectively (Kiyono and Fukuyama, 2004). It has been revealed that the interaction of $\alpha4\beta7$ integrin on lymphocytes and mucosal addressin cell adhesion molecule 1 (MAdCAM-1) on HEVs is essential for lymphocyte homing to PPs (Nakache et al., 1989; Berlin et al., 1993). In contrast, adhesion molecules important for lymphocyte homing to NALT in vivo have yet to be identified. Considering that nasal vaccination protocols have achieved effective immune reactions (Imaoka et al., 1998; Kurono et al., 1999; Imai et al., 2005) and that various antigens, including pollen and house dust, that are taken up from the nasal mucosal barrier often cause Th2-mediated allergic rhinitis characterized by antigen-specific IgE production and nasal symptoms, such as sneezing (Gelfand, 2004), understanding the molecular mechanisms of cellular trafficking to NALT and how to manipulate them is clinically important. It was previously reported that PNAd is expressed in NALT HEVs (Csencsits et al., 1999), but the significance of its expression for lymphocyte homing in vivo remains elusive.

In the present study, we sought to determine the role of PNAd in lymphocyte homing to NALT and in allergic immune responses against inhaled antigens using sulfotransferase DKO mice. The results of this study demonstrate that expression of PNAd is completely abrogated in the NALT of DKO mice and that lymphocyte homing to NALT is significantly diminished in these mutant mice. We also found that IgE production and nasal symptoms of rhinopathy are suppressed in DKO mice in relation to a reduction in IL-4 and increases in IL-10 and $CD4^+CD25^+$ regulatory T cells (T_{reg} cells). Moreover, we

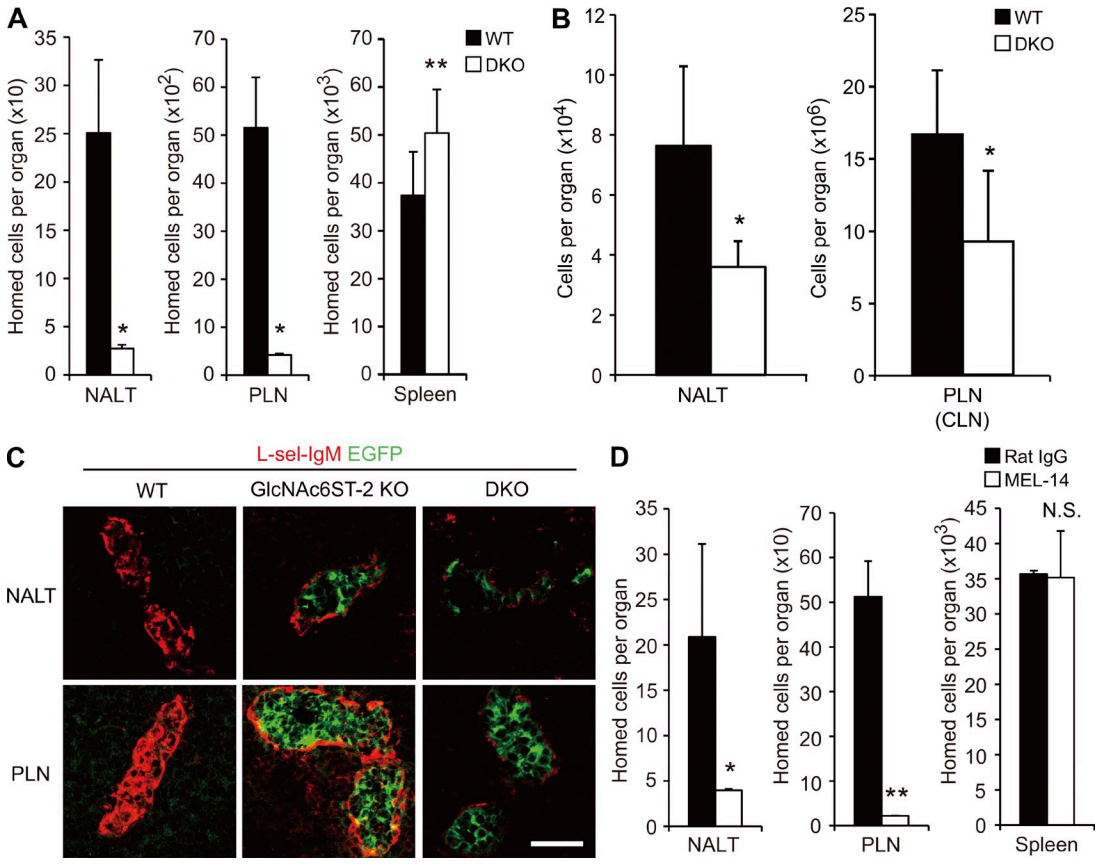

Figure 2. Reduction of lymphocyte homing to NALT in DKO mice. (A) Lymphocyte homing to secondary lymphoid organs. Lymphocytes labeled with CFSE were injected into tail veins of WT and DKO mice, and fluorescent lymphocytes from NALT, PLNs, and spleen were quantified by flow cytometry. Data from four separate experiments were pooled. $n = 11–12$. Each bar represents the mean ± SD. *, $P < 0.001$; **, $P < 0.02$ versus WT mice. (B) The total numbers of cells in NALT and PLNs (CLNs) from WT and DKO mice were counted. $n = 3–14$. Each bar represents the mean ± SD. *, $P < 0.01$ versus WT mice. (C) Expression of L-selectin ligands. Frozen sections of NALT and PLNs were stained with L-selectin–IgM (L-sel-IgM, red). Green fluorescence is from the GlcNAc6ST-2-EGFP chimeric protein. Bar, 30 µm. Data are representative of three independent experiments. (D) Inhibition of lymphocyte homing in DKO mice by MEL-14. CFSE-labeled lymphocytes preincubated with MEL-14 or control rat IgG were injected into the tail vein of each DKO mouse. Each bar represents the mean ± SD. $n = 3$. *, $P < 0.05$; **, $P < 0.005$ versus rat IgG-injected mice. N.S., not significant. Data are representative of two independent experiments.

found that $CD4^+CD25^+$ T_{reg} cells are recruited to NALT in a manner less dependent on the L-selectin–PNAd interaction and partially dependent on P-selectin glycoprotein ligand 1 (PSGL-1) and CD44. Our results suggest that blocking PNAd-mediated lymphocyte homing to NALT could serve as a therapeutic target for allergic rhinitis induced by inhaled antigens.

RESULTS

Expression of PNAd, but not MAdCAM-1, in NALT HEVs

An immunofluorescence study using the antibody MECA-79 (Streeter et al., 1988) indicated that PNAd is strongly expressed in the NALT HEVs of C57BL/6 WT mice (Fig. 1 A). In GlcNAc6ST-2–deficient (KO) mice, staining with MECA-79 was observed only on the abluminal side of NALT HEVs, surrounding green fluorescence derived from EGFP-GlcNAc6ST-2 fusion proteins, which accumulate in the Golgi apparatus of HEVs (Hiraoka et al., 2004; Kawashima et al., 2005). Moreover, no staining with MECA-79 was observed in NALT HEVs in DKO mice, indicating that the two sulfotransferases are essential for the sulfation of PNAd in NALT HEVs. Strong staining with the antibody MECA-367, which reacts with MAdCAM-1 (Nakache et al., 1989), was observed in PPs but not in NALT or PLNs (Fig. 1 B). Thus, although NALT is a MALT similar to PPs, its addressin expression pattern is more similar to that of PLN.

Roles of PNAd in lymphocyte homing to NALT

To assess the role of PNAd expressed in NALT HEVs, we next performed a lymphocyte homing assay (Fig. 2 A). In DKO mice, lymphocyte homing to NALT and PLNs was diminished by 90% compared with that observed in WT mice, indicating that PNAd plays a critical role in lymphocyte homing to NALT and PLNs. Consistent with that result, the total cell number in NALT was reduced by 50% in DKO mice, similar to what was observed in PLNs (cervical LNs [CLNs]; Fig. 2 B).

To determine the specificity of the residual lymphocyte homing to NALT observed in DKO mice, we next examined

Table I. Number of lymphocyte subpopulations in NALT and PLN in WT and DKO mice

Cell population	Cells in NALT[a]		Cells in PLN (CLN; ×10³)[a]	
	WT	DKO	WT	DKO
$CD3^+$	8,205 ± 470 (10.7 ± 0.6)	7,560 ± 360 (21.0 ± 1.0)	9,413 ± 380 (56.4 ± 2.3)	7,081 ± 199 (76.6 ± 2.2)
$CD3^+CD4^+$	6,673 ± 503 (8.7 ± 0.7)	5,319 ± 105 (14.8 ± 0.3)	4,809 ± 86 (28.8 ± 0.5)	4,053 ± 237 (43.9 ± 2.6)
$CD3^+CD4^+CD25^-$	5,955 ± 632 (7.8 ± 0.8)	3,964 ± 346 (11.0 ± 1.0)	4,232 ± 41 (25.3 ± 0.2)	3,548 ± 239 (38.4 ± 2.6)
$CD3^+CD4^+CD25^+$	718 ± 129 (0.94 ± 0.17)	1,355 ± 274 (3.8 ± 0.76)	576 ± 47 (3.5 ± 0.28)	505 ± 14 (5.5 ± 0.15)
$CD3^+CD8^+$	1,531 ± 288 (2.0 ± 0.38)	2,241 ± 283 (6.2 ± 0.79)	4,604 ± 311 (27.6 ± 1.9)	3,028 ± 262 (32.8 ± 2.8)
$CD19^+$	64,903 ± 364 (85.1 ± 0.5)	24,575 ± 663 (68.3 ± 1.8)	6,365 ± 396 (38.1 ± 2.4)	1,727 ± 182 (18.7 ± 2.0)
Others	3,193 ± 112 (4.2 ± 0.15)	3,865 ± 999 (10.7 ± 2.8)	923 ± 19 (5.5 ± 0.11)	432 ± 42 (4.7 ± 0.45)

Numbers in the parentheses represent the mean percentage ± SD of cells in each lymphoid organ.
[a]Values represent means ± SD of cell numbers in NALT and CLN per mouse ($n = 3$).

whether L-selectin ligands could still be detected in DKO mice. Immunofluorescence study using an L-selectin–IgM chimeric molecule indicated that L-selectin ligand expression in NALT was significantly lower in the KO mice (Fig. 2 C). Only faint staining with L-selectin–IgM was observed in NALT in the DKO mice, suggesting that a very small amount of L-selectin ligand activity remains in the DKO mice. Consistent with this notion, pretreatment of fluorescence-labeled lymphocytes with MEL-14, a mAb that blocks L-selectin function (Gallatin et al., 1983), significantly inhibited the residual lymphocyte homing to NALT observed in the DKO mice, similar to what was observed in PLNs (Fig. 2 D). These results indicate that PNAd plays a major role in lymphocyte homing to NALT, although a small amount of L-selectin ligands are expressed in the NALT of DKO mice.

Changes in lymphocyte subpopulations in DKO mice

We next examined lymphocyte subpopulations in NALT by flow cytometry (Table I). In DKO mice, $CD19^+$ B cells were more significantly diminished than $CD3^+$ T cells in NALT. To examine the possibility that chemokine expression might differ in WT and DKO mice in NALT, we performed immunohistochemical staining using anti-chemokine antibodies against CCL21, which primarily attracts T cells, as shown by the analysis of *plt* (paucity of LN T cell) mutant mice (Luther et al., 2000; Nakano and Gunn, 2001) and CXCL12, which is important for B cell homing (Okada et al., 2002; Fig. S1). We did not see a significant difference in chemokine expression between WT and DKO mice. These results suggest that the decrease of B cells in DKO mice was not explained by the difference in chemokine expression but might be explained by the fact that B cells express lower levels of L-selectin compared with T cells and that B cell homing is more susceptible to the reduction of L-selectin ligands in HEVs than that of T cells (Gauguet et al., 2004; Uchimura et al., 2005).

Another notable difference was that $CD4^+CD25^-$ T cells were decreased in DKO mice, whereas $CD4^+CD25^+$ and $CD8^+$ T cells were increased in DKO mice (Table I). In particular, the ratio of $CD4^+CD25^+$ T cells among total lymphocytes in NALT was approximately four times higher in DKO mice than in WT mice (Table I and Fig. 3 A). Most of the $CD4^+CD25^+$ T cells expressed Foxp3 (Fig. 3 B), a T_{reg} cell–specific transcription factor (Hori et al., 2003), indicating that most of the $CD4^+CD25^+$ T cells observed in Fig. 3 A were T_{reg} cells. Notably, $CD4^+CD25^+$ T_{reg} cells expressing a lower level of L-selectin (CD62L) were more enriched in the NALT and spleen in DKO mice (Fig. 3 C). A short-term homing assay indicated that the homing of $CD4^+CD25^-$ conventional T cells (T_{conv} cells) to NALT and PLNs was significantly decreased in DKO mice. Similarly, homing of $CD4^+CD25^+$ T_{reg} cells to PLNs was also significantly decreased in DKO mice. In contrast, homing of $CD4^+CD25^+$ T_{reg} cells to NALT in DKO mice was almost comparable with that observed in WT mice (Fig. 3 D). Collectively, these results suggest that homing of $CD4^+CD25^+$ T_{reg} cells to NALT is less dependent on an L-selectin–PNAd interaction than that of $CD4^+CD25^-$ T_{conv} cells to NALT and those of $CD4^+CD25^+T_{reg}$ and $CD4^+CD25^-$ T_{conv} cells to PLNs.

Roles of PSGL-1 and CD44 in the homing of $CD4^+CD25^+$ T_{reg} cells to NALT

Consistent with the results in the previous section, the short-term homing assay indicated that the anti–L-selectin mAb MEL-14 significantly inhibited homing of $CD4^+CD25^-$ T_{conv} cells to NALT but only partially inhibited that of $CD4^+CD25^+$ T_{reg} cells (Fig. 4 A). In contrast, homing of both $CD4^+CD25^-$ T_{conv} and $CD4^+CD25^+$ T_{reg} cells to PLNs was significantly inhibited by MEL-14 (Fig. 4 B).

To identify the homing receptors other than L-selectin that mediate the homing of $CD4^+CD25^+$ T_{reg} cells to NALT, we next examined whether PSGL-1 (Alon et al., 1995; Moore et al., 1995) and CD44 (DeGrendele et al., 1996), the other carbohydrate-dependent rolling receptors on lymphocytes, might play a role. As shown in Fig. 4 (A and B), an anti–PSGL-1 blocking mAb 4RA10 (Frenette et al., 2000) and an anti–P-selectin mAb RB40.34 (Bosse and Vestweber, 1994) partially inhibited homing of $CD4^+CD25^+$ T_{reg} cells to NALT but not to PLNs. Consistently, real-time quantitative PCR analysis using FACS-sorted $CD4^+CD25^-$ T_{conv} cells and $CD4^+CD25^+$ T_{reg} cells (Fig. 4 C) showed that expression of the mRNA for fucosyltransferase-VII, which is required for a posttranslational modification of PSGL-1 required for its interaction

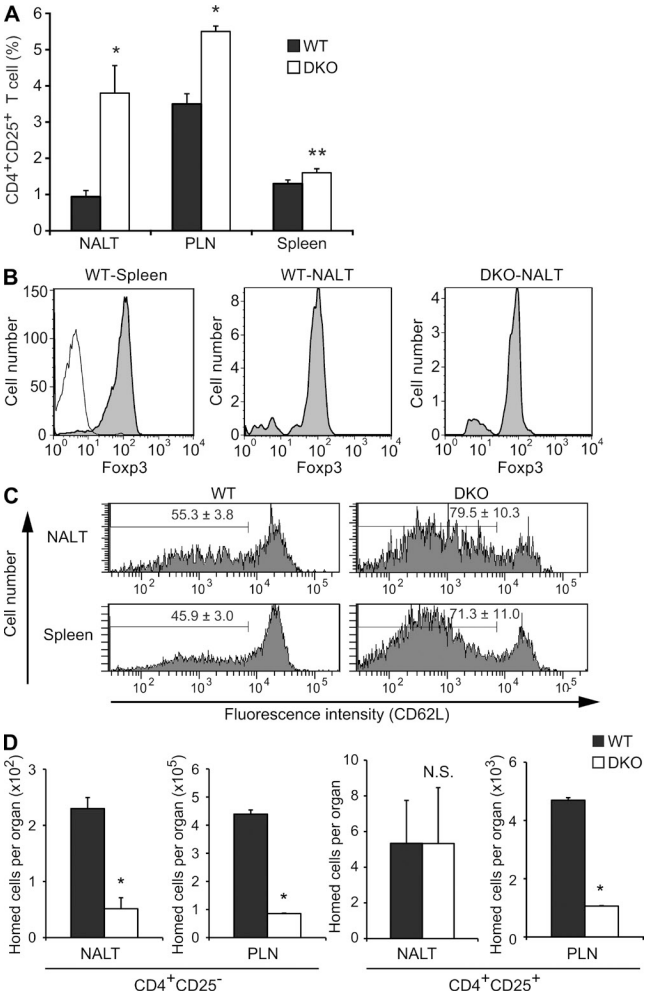

Figure 3. Accumulation of CD4⁺CD25⁺ T_{reg} cells in the NALT of DKO mice. (A) Frequency of CD4⁺CD25⁺ T_{reg} cell subsets. NALT, PLN (CLN), and splenic lymphocytes from WT and DKO mice were stained with APC-conjugated anti-CD3, APC-Cy7–conjugated anti-CD4, and FITC-conjugated anti-CD25 mAbs and analyzed by flow cytometry. The vertical axis represents the percentage of CD4⁺CD25⁺ T cells relative to total lymphocytes. Each bar represents the mean ± SD. $n = 3$. *, $P < 0.002$; **, $P < 0.01$. (B) Foxp3 staining of gated CD4⁺CD25⁺ T cells from the spleen (WT-Spleen) and the NALT (WT-NALT) of WT mice and from the NALT of DKO mice (DKO-NALT, shaded). Staining of gated CD4⁺CD25⁺ T cells from WT spleens with an isotype control (thin line). (C) CD62L expression. The expression of CD62L on gated CD4⁺CD25⁺ T_{reg} cells from the NALT and the spleen of WT and DKO mice was examined by flow cytometry. The number of each panel indicates the mean percentage ± SD of cells in the gate ($n = 3$). $P < 0.01$. (D) Homing of CD4⁺CD25⁻ T_{conv} cells and CD4⁺CD25⁺ T_{reg} cells. CFSE-labeled lymphocytes were injected intravenously into WT or DKO mice. 2 h after injection, lymphocytes from NALT and PLNs (CLNs) were stained with APC-Cy7–conjugated anti-CD4 and APC-conjugated anti-CD25 mAbs to differentiate CD4⁺CD25⁻ T_{conv} cell and CD4⁺CD25⁺ T_{reg} cell homing after gating CFSE-positive cell fractions. Each bar represents the mean ± SD. $n = 3$. *, $P < 0.01$ versus WT. N.S., not significant. Data are representative of two (A, B, and D) or three (C) independent experiments.

with P-selectin (Snapp et al., 1997), was 12× higher in CD4⁺CD25⁺ T_{reg} cells than in CD4⁺CD25⁻ T_{conv} cells (Fig. 4 D). The expression of PSGL-1 core protein was also slightly higher in CD4⁺CD25⁺ T_{reg} cells than in CD4⁺CD25⁻ T_{conv} cells. In addition, RT-PCR analysis, using total RNA from HEV cells from NALT purified by immunomagnetic selection using HEV-specific mAb S2 (Hirakawa et al., 2010), indicated that P-selectin mRNA was expressed in NALT HEVs (Fig. 4 E).

To determine the role of CD44, we next examined the effects of the anti-CD44 mAb IM7, which blocks CD44-mediated lymphocyte rolling on hyaluronic acid (HA)–coated dishes (DeGrendele et al., 1996). As shown in Fig. 4 A, IM7 significantly inhibited the homing of CD4⁺CD25⁺ T_{reg} cells to NALT. IM7 also slightly inhibited the homing of CD4⁺CD25⁺ T_{reg} cells to PLNs (Fig. 4 B). Consistent with these findings, expression of HA, a ligand for CD44 (Aruffo et al., 1990), was detected in the NALT and PLN HEVs (Fig. 4 F). In addition, CD4⁺CD25⁺ T_{reg} cells expressed CD44 more abundantly than CD4⁺CD25⁻ T_{conv} cells (Fig. 4 G). Furthermore, treatment of CD4⁺CD25⁺ T_{reg} cells with a mixture of MEL-14, 4RA10, and IM7 more significantly inhibited the homing of these cells to NALT than treatment with the individual mAbs (Fig. 4 A). In contrast, treatment with the mixture of mAbs failed to show any additive inhibitory effects compared with that with MEL-14 alone regarding the homing of CD4⁺CD25⁻ T_{conv} cells to NALT. Collectively, these results indicate that the homing of CD4⁺CD25⁺ T_{reg} cells to the NALT is less dependent on L-selectin but is more dependent on PSGL-1 and CD44 compared with the homing of CD4⁺CD25⁻ T_{conv} cells to the NALT.

Roles of PNAd in allergic immune responses after intranasal immunization

As described in the previous section, NALT is a mucosal immune tissue where immune responses against antigens from the nasal mucosal barrier occur. To determine if PNAd is involved in the allergic immune responses in NALT, we next immunized WT and DKO mice intranasally with OVA. Production of OVA-specific serum IgE in DKO mice was about three times lower than that in WT mice (Fig. 5 A). OVA-specific serum IgG and nasal wash IgA were not significantly different between the two genotypes of mice (Fig. 5, B and C). Consistently, the number of sneezes after intranasal immunization with OVA was lower in DKO mice than in WT mice (Fig. 5 D). We further examined the effects of L-selectin blockade on allergic responses using mAb MEL-14. As shown in Fig. S2, MEL-14 suppressed OVA-specific serum IgE production and sneezing to a degree almost comparable with that observed in DKO mice, indicating that blockade of the L-selectin–PNAd adhesion pathway suppresses allergic immune responses after intranasal immunization. In addition, immunofluorescence studies revealed that HA was expressed in NALT HEVs in WT and DKO mice after intranasal immunization with OVA (Fig. S3), which could partly mediate trafficking of T_{reg} cells to NALT, as described in the previous section.

Cytokine production in NALT after intranasal immunization

To determine the molecular basis for the alleviation of allergic immune responses in DKO mice after intranasal immunization,

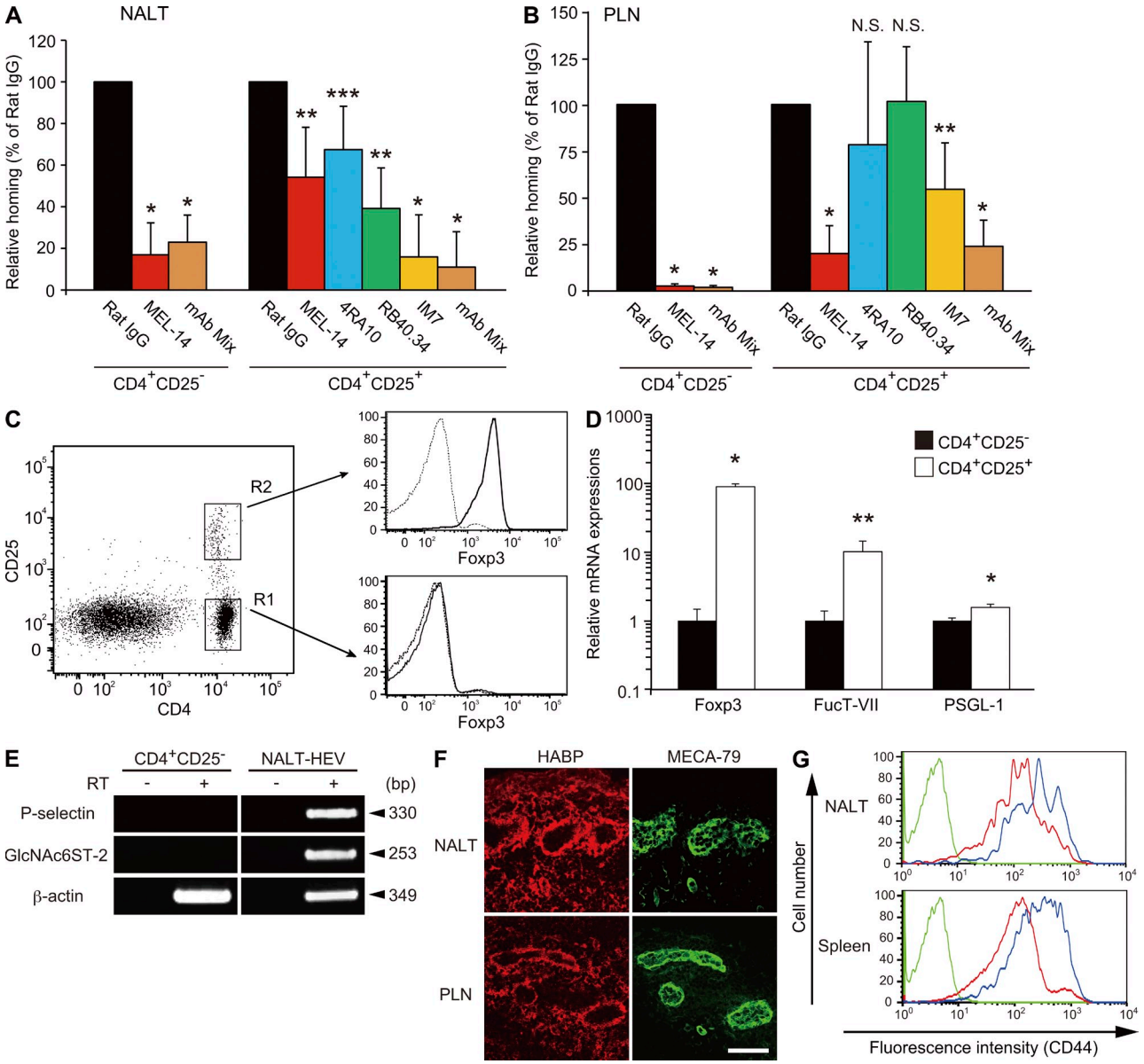

Figure 4. Homing of CD4⁺CD25⁺ T_{reg} cells to NALT is partially dependent on PSGL-1 and CD44. (A and B) CFSE-labeled CD4⁺CD25⁻ T_{conv} cells and CMTMR-labeled CD4⁺CD25⁺ T_{reg} cells were treated with or without neutralizing mAb, mixed at a ratio of 1:1, and injected into WT mice intravenously. 2 h later, lymphocytes from the NALT (A) and the PLNs (CLNs; B) were collected and analyzed by flow cytometry after gating on the CFSE- or CMTMR-positive cell fractions. The neutralizing mAbs used were anti–L-selectin (MEL-14), anti–PSGL-1 (4RA10), anti–P-selectin (RB40.34), and anti-CD44 (IM7), and rat IgG as a control. In some experiments, cells were treated with a mixture of MEL-14, 4RA10, and IM7 (mAb Mix). Each bar represents the mean ± SD. $n = 4$. *, $P < 0.002$; **, $P < 0.01$; ***, $P < 0.03$. N.S., not significant. Rat IgG-treated control was set as 100%. In A and B, data from four separate experiments were pooled. (C) FACS sorting and Foxp3 staining. FACS-sorted CD4⁺CD25⁺ T_{reg} cells (R2) and CD4⁺CD25⁻ T_{conv} cells (R1) from WT mice were stained with PE-conjugated anti–mouse Foxp3 mAb (bold line) or PE-conjugated isotype control (thin line) using a T_{reg} cell staining kit and analyzed by flow cytometry. Representative data from two independent experiments are shown. (D) Real-time quantitative PCR analysis. Total RNA from FACS-sorted CD4⁺CD25⁻ T_{conv} cells and CD4⁺CD25⁺ T_{reg} cells was subjected to real-time PCR analysis for Foxp3, fucosyltransferase-VII (FucT-VII), and PSGL-1. Each bar represents the mean ± SD. $n = 3$. *, $P < 0.005$; **, $P < 0.02$. Representative data from three independent experiments are shown. (E) RT-PCR analysis of P-selectin expression in NALT HEVs. Total RNA was purified from CD4⁺CD25⁻ T_{conv} cells (CD4⁺CD25⁻) and the mAb S2⁺ HEV cells from NALT (NALT-HEV). Single-stranded cDNA was prepared from the total RNA in the presence (+) or absence (−) of RT and was subjected to PCR using primers for P-selectin, GlcNAc6ST-2, and β-actin. Sizes of the PCR products are indicated on the right. Data are representative of two independent experiments. (F) Expression of HA in NALT and PLN HEVs. Frozen sections of NALT and PLNs from WT mice were costained with DyLight 488–conjugated MECA-79 (green), and biotinylated HA-binding protein and Alexa Fluor 594–conjugated streptavidin (red). Bar, 50 µm. Data are representative of three independent experiments. (G) CD44 expression on T_{conv} and T_{reg} cells. The expression of CD44 on gated CD4⁺CD25⁻ T_{conv} (red line) and CD4⁺CD25⁺ T_{reg} cells (blue line) from the NALT and spleen of WT mice was examined by flow cytometry. The green line represents unstained lymphocytes without mAb incubation. Data are representative of two independent experiments.

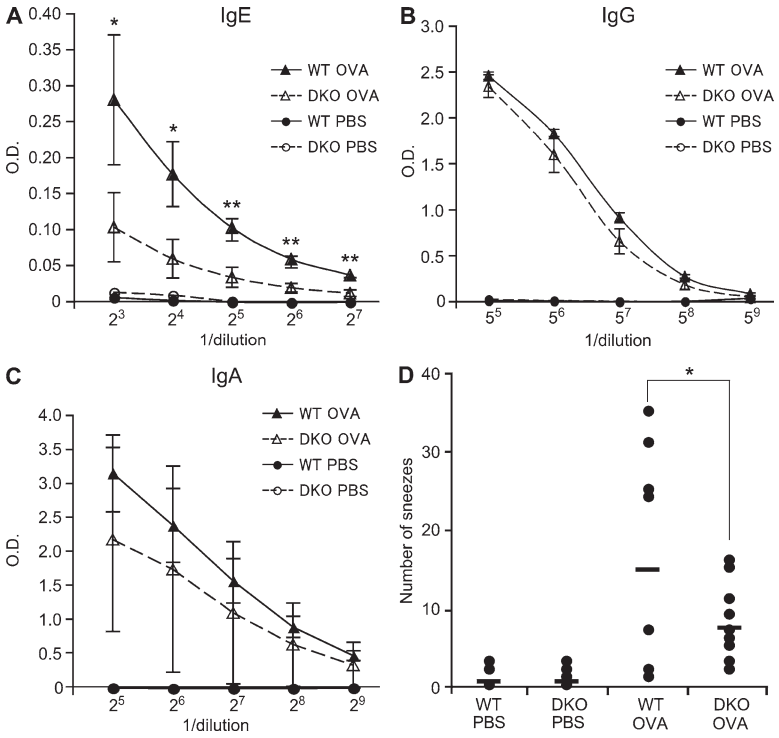

Figure 5. DKO mice exhibit reduced OVA-specific IgE production and attenuated nasal symptoms. (A, B, and C) ELISA for OVA-specific IgE (A) and IgG (B) in serum and IgA in nasal wash (C). WT and DKO mice were immunized intranasally with OVA and CT in PBS (closed and open triangles, respectively) or with PBS alone (closed and open circles, respectively) on days 0, 7, and 14, and OVA-specific antibodies were measured by ELISA on day 21. Error bars represent the SD of triplicate determinations. *, $P < 0.05$; **, $P < 0.01$. Data are representative of four independent experiments. (D) Nasal symptoms after intranasal immunization. WT and DKO mice were intranasally immunized with OVA and CT on days 0, 7, and 14. On day 21, mice were intranasally challenged with PBS alone or OVA and CT in PBS. 2 min later, the number of sneezes was counted for 5 min. Each horizontal bar represents the mean of the values obtained from 6–10 animals. *, $P = 0.07$. Data from three separate experiments were pooled.

we next prepared total RNA from NALT after immunization and performed real-time quantitative PCR analysis (Fig. 6). The induction of the humoral immunity-related Th2 cytokine IL-4, which is a major mediator of IgE class switching in B cells (Zhu and Paul, 2008), was observed in WT mice, but not in DKO mice, after intranasal immunization with OVA. In contrast, more mRNA for the immune-suppressive cytokine IL-10 was detected in DKO mice than in WT mice after immunization, consistent with the higher amount of Foxp3 mRNA and the higher ratio of T_{reg} cells recruited to NALT in DKO mice, as shown in the previous section. Only a slight increase in TGF-β was observed in the NALT of DKO mice, suggesting that IL-10–producing, but not TGF-β–producing, T_{reg} cells increased in the NALT of DKO mice. The amount of mRNA for the Th1-related cytokine IFN-γ and the Th17-related cytokine IL-17A in the NALT in DKO mice was not statistically different from that in WT mice (unpublished data).

DISCUSSION

In this study, we found that PNAd plays an essential role in lymphocyte recruitment to a mucosal lymphoid tissue, NALT, and in the allergic immune responses after intranasal immunization. Previous studies from our laboratory and others indicated that PNAd plays an essential role in lymphocyte trafficking to PLNs but not to the PP mucosal lymphoid tissue (Kawashima et al., 2005; Uchimura et al., 2005). We also found that PNAd is involved in the regulation of lymphocyte subpopulations and the cytokine environment, both of which are critical for balancing immune responses in NALT.

Csencsits et al. (1999) showed that NALT HEVs of BALB/c mice were reactive with both MECA-79 and MECA-367 antibodies and that binding of lymphocytes to NALT HEVs was significantly inhibited by MEL-14, but not by MECA-367, in a Stamper-Woodruff ex vivo cell binding assay. Although the

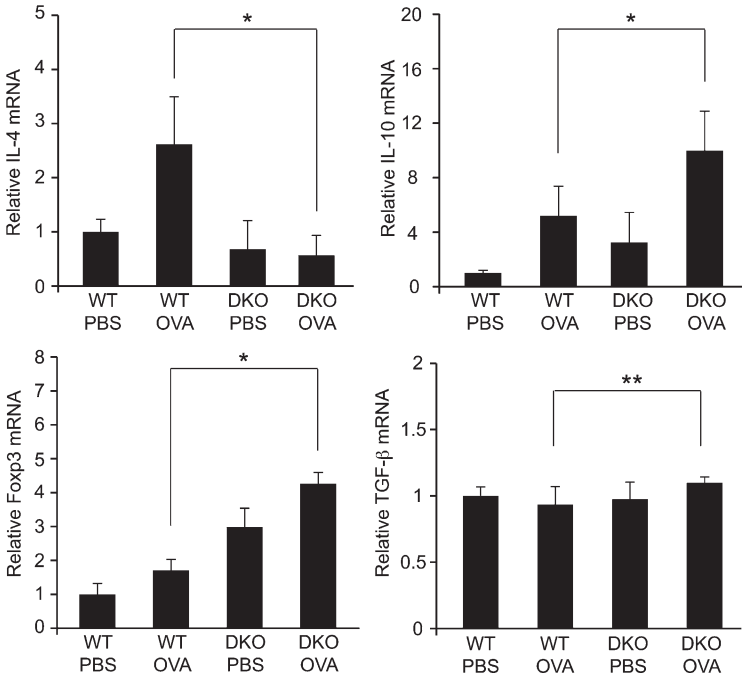

Figure 6. Real-time quantitative PCR analysis of various mRNAs in NALT after immunization. Real-time quantitative PCR analysis was performed using total RNA samples from NALT collected on day 15 from WT or DKO mice that had been immunized with OVA and CT in PBS (OVA) or with PBS alone (PBS) on days 0, 7, and 14. Each bar represents the mean ± SD. $n = 3–7$. *, $P < 0.02$; **, $P < 0.05$. N.S., not significant. Data from two separate experiments were pooled.

latter finding is consistent with our in vivo results, the former is not consistent with our results showing that the NALT HEVs of C57BL/6 mice were exclusively reactive with MECA-79. To solve this discrepancy, we stained the NALT HEVs of BALB/c mice with MECA-367 and detected reactivity in some HEVs with this antibody (Fig. S4). This result suggests that the strain difference accounts for the differential expression pattern of MECA-367 antigens. It is of note that all of the NALT HEVs in BALB/c mice expressed MECA-79 antigen, whereas ∼63% of them coexpressed MECA-367 antigen (Csencsits et al., 1999), suggesting that even though MECA-367 antigen is expressed in NALT HEVs in BALB/c mice, PNAd should play a major role in lymphocyte recruitment to NALT in these mice.

L-selectin–IgM staining and a blocking experiment with MEL-14 antibody indicated that a faint but detectable amount of L-selectin ligands remain in NALT HEVs in DKO mice (Fig. 2). It seems likely that unsulfated sialyl Lewis X structures support the residual L-selectin–dependent lymphocyte homing to NALT in DKO mice because this carbohydrate structure binds to L-selectin in vitro (Foxall et al., 1992). In support of this notion, the staining of NALT sections from WT and DKO mice with the recently generated antisulfated glycan mAbs S1 and S2, which specifically recognize GlcNAc-6-*O*-sulfated carbohydrate structures (Hirakawa et al., 2010), indicated that GlcNAc-6-*O*-sulfation was completely eliminated from the NALT HEVs of DKO mice (Fig. S5). In addition, a carbohydrate structural analysis of PLN HEV–derived glycoproteins performed in our previous study indicated that 6-sulfo sialyl Lewis X structures were almost completely abrogated, whereas unsulfated sialyl Lewis X structures were significantly enhanced in DKO mice (Kawashima et al., 2005).

Unlike GlcNAc6ST-2, GlcNAc6ST-1 is widely expressed in various tissues (Uchimura et al., 1998). Thus, one may argue that the lack of GlcNAc6ST-1 in immune cells in DKO mice might have some functional immunological relevance. However, although GlcNAc6ST-1 is relatively strongly expressed in various organs such as the brain, eyes, lung, and pancreas, it is not expressed in bone marrow and is only very weakly expressed in the thymus and spleen (Uchimura et al., 1998), suggesting that immune cells do not express GlcNAc6ST-1. In addition, our previous results indicated that immune responses were unaffected in GlcNAc6ST-1 single KO mice (Kawashima et al., 2005). Thus, we think that it is unlikely that the lack of GlcNAc6ST-1 in immune cells in DKO mice has any functional relevance regarding immune responses in NALT, although we cannot completely rule out this possibility.

Importantly, the homing of $CD4^+CD25^+$ T_{reg} cells to NALT was less dependent on the L-selectin–PNAd interaction than that of $CD4^+CD25^-$ T_{conv} cells (Fig. 4). Furthermore, we found that the homing of $CD4^+CD25^+$ T_{reg} cells to NALT was also dependent on PSGL-1 and CD44. It was reported that $CD4^+CD25^+$ T_{reg} cell migration to PLNs requires L-selectin (Venturi et al., 2007). The same paper also reported that 40% of the $CD4^+$ T cells in the PLNs of L-selectin–deficient mice are T_{reg} cells, suggesting that adhesion molecules other than L-selectin might mediate the homing of $CD4^+CD25^+$ T_{reg} cells to PLNs in these mutant mice. It was reported that *plt* mutant mice, which have mutations in CCL21 (produced by stromal cells and HEVs) and CCL19 (Luther et al., 2000; Nakano and Gunn, 2001), showed aggravated allergic symptoms associated with a reduction in T_{reg} cells expressing CCR7, the receptor for CCL21 (Yoshida et al., 1998) and CCL19 (Yoshida et al., 1997), in NALT, showing the importance of the chemokines CCL21 and CCL19 for T_{reg} cell homing to NALT (Takamura et al., 2007). However, as far as we know, no previous reports have shown the importance of adhesion molecules for T_{reg} cell homing to NALT in vivo. It has been well discussed that appropriate localization is indispensable for the appropriate function of T_{reg} cells in vivo (Huehn and Hamann, 2005). We believe that the results of the present study have clarified, at least in part, the address codes for T_{reg} cell migration, and they should permit the function of T_{reg} cells to be manipulated in the future, with relevance for host responses to tumors, transplant rejection, autoimmunity, and allergies (Sakaguchi, 2005).

Flow cytometric analysis indicated that $CD4^+CD25^+$ T_{reg} cells expressing lower levels of L-selectin accumulate not only in NALT but also in the spleen of DKO mice (Fig. 3 C), probably because $CD4^+CD25^+$ T_{reg} cells expressing lower levels of L-selectin are preferentially maintained in DKO mice. Considering a previous study that fibroblastic reticular cells in LNs provide survival signals through IL-7 to naive T cells (Link et al., 2007), one possible explanation for why $CD4^+CD25^+$ T_{reg} cells expressing lower levels of L-selectin accumulate in DKO mice is that naive $CD4^+CD25^+$ T_{reg} cells that can migrate to secondary lymphoid organs in an L-selectin–independent manner might be better maintained in DKO mice. Alternatively, because some $CD4^+CD25^+$ T_{reg} cells sequentially migrate from inflamed tissues to draining LNs (Zhang et al., 2009) and some others are induced by a commensal bacterium of the intestinal microbiota (Round and Mazmanian, 2010; Atarashi et al., 2011), the $CD4^+CD25^+$ T_{reg} cells activated in the inflamed mucosa or induced in the intestines expressing lower levels of L-selectin might accumulate in DKO mice.

Another notable observation in relation to the homing of $CD4^+CD25^+$ T_{reg} cells is that homing of these cells to NALT was less dependent on L-selectin compared with the homing to PLNs (Fig. 4, A and B). In immunofluorescence studies, the MECA-79 staining intensities in NALT HEVs and PLN HEVs were indistinguishable under the staining conditions we used, suggesting that PNAd in these lymphoid organs is modified with a similar level of sulfated extended core 1 *O*-glycans. However, because the other core structures, such as core 2 *O*-glycans (Hiraoka et al., 2004) and *N*-glycans (Mitoma et al., 2007), as well as fucosylation (Homeister et al., 2001) and sialylation (Rosen et al., 1985) of PNAd, are also important for L-selectin binding, one possible explanation is that some of these glycosylation events might be less efficient in NALT HEVs than in PLN HEVs.

Although L-selectin ligand activity was not completely abrogated in DKO mice, IgE production and the number of sneezes after intranasal immunization with OVA were lower

in DKO mice (Fig. 5). These results suggest that complete blockade of the PNAd-mediated adhesion pathway, which is too difficult to attain in clinical settings, seems not to be required to suppress allergic symptoms. Our data collectively support the model that T_{reg} cells accumulate in NALT in DKO mice because of their decreased dependency on the L-selectin–PNAd adhesion pathway and their greater dependency on PSGL-1–P-selectin and CD44–HA adhesion pathways, and they thereby create an immune-suppressive environment in the NALT (Fig. S6). Consistent with this model, we detected higher levels of the immunosuppressive cytokine IL-10 (Fig. 6), which is known to be secreted from T_{reg} cells, in DKO mice compared with WT mice, suggesting that IL-10 production explains, at least in part, why allergic immune responses are reduced in DKO mice. Collectively, our results indicate that blocking PNAd-mediated lymphocyte recruitment could serve as a novel therapeutic approach for modulating allergic rhinitis.

MATERIALS AND METHODS

Mice. GlcNAc6ST-2 KO and GlcNAc6ST-1 and GlcNAc6ST-2 DKO mice were backcrossed at least five generations to C57BL/6 mice and maintained as described previously (Kawashima et al., 2005). Genomic DNA was isolated from mouse tails and used for PCR genotyping. C57BL/6 mice were used as WT controls throughout the study. BALB/c mice were purchased from Japan SLC. Mice were treated in accordance with the guidelines of the Animal Research Committee of the University of Shizuoka.

Immunohistochemistry. 7-µm-thick frozen sections were fixed with ice-cold acetone and incubated with PBS containing 3% BSA (Sigma-Aldrich). The sections were incubated with 10 µg/ml MECA-79 or MECA-367 (BD) primary antibody, followed by 10 µg/ml biotinylated secondary antibody (mouse anti–rat IgM [BD] or goat anti–rat IgG $F(ab')_2$ fragment [Rockland Immunochemical]). In some experiments, sections were incubated with L-selectin–IgM (Hiraoka et al., 2004), 10 µg/ml goat anti–mouse CCL21 (R&D Systems), or 10 µg/ml goat anti–mouse CXCL12 (Santa Cruz Biotechnology, Inc.), followed by 2 µg/ml Alexa Fluor 594–labeled goat anti–human IgM (Invitrogen) or 3 µg/ml biotinylated rabbit anti–goat IgG (Vector Laboratories). Binding of biotinylated secondary antibodies was detected with 2.5 or 5 µg/ml Texas red avidin D (Vector Laboratories) or 1 µg/ml Alexa Fluor 594–conjugated streptavidin (Invitrogen). To detect HA expression on HEVs, frozen sections were stained with 2.5 µg/ml DyLight 488–conjugated MECA-79 and 5 µg/ml of biotinylated HA-binding protein (Seikagaku Kogyo Co., Ltd), followed by 0.5 µg/ml Alexa Fluor 594–conjugated streptavidin. After incubation, sections were mounted with GEL/MOUNT (Biomeda Corp.). In all experiments, isotype-matched antibodies were used as negative controls. Data were acquired on a confocal laser-scanning microscope (LSM510 META; Carl Zeiss) using a 40× water immersion objective.

Lymphocyte homing assay. Lymphocyte homing was assayed as described previously (Hiraoka et al., 2004; Kawashima et al., 2005) with some modifications. In brief, lymphocytes prepared from the spleens and mesenteric LNs (MLNs) of WT mice were labeled with 1 µM CFSE (Invitrogen) and injected intravenously into WT or mutant mice (2.7×10^7 lymphocytes/mouse). 1 h after injection, the fraction of $CFSE^+$ cells in a cell suspension of recipient lymphoid organs was determined by flow cytometry on a FACSCanto II (BD). All data were analyzed with FACS Diva software (BD) and FlowJo software (Tree Star, Inc). For the L-selectin inhibition experiment, CFSE-labeled cells were preincubated for 15 min with 100 µg/ml control rat IgG (Sigma-Aldrich) or MEL-14 (Beckman Coulter), and the mixture of cells and antibodies (300 µl/mouse) was injected intravenously into mice. For T_{reg} cell homing assays, CFSE-labeled PLN and MLN lymphocytes were injected intravenously (2.5×10^7 lymphocytes/mouse) into WT and DKO mice. After 2 h, lymphocyte suspensions of recipient lymphoid organs were stained with allophycocyanin (APC)-conjugated anti–mouse CD25 (PC61.5; eBioscience) and APC–cyanine-7 (Cy7)–conjugated anti–mouse CD4 (GK1.5; BioLegend) to differentiate homing of $CD4^+CD25^-$ T_{conv} cells and $CD4^+CD25^+$ T_{reg} cells. To determine the effects of various mAbs on T_{reg} and T_{conv} cell homing, $CD4^+CD25^+$ T_{reg} cells and $CD4^+CD25^-$ T_{conv} cells were purified from PLNs, MLNs, and spleens of WT mice using a $CD4^+CD25^+$ T_{reg} cell isolation kit (>95% purity; Miltenyi Biotec), labeled with 0.75 µM CMTMR (5-(and-6)-(((4-chloromethyl)benzoyl)amino)tetramethylrhodamine; Lonza) and 0.05 µM CFSE, respectively, and treated with 33 µg/ml (10 µg/mouse) of control rat IgG or anti–PSGL-1 (4RA10; BD), anti–P-selectin (RB40.34; BD), anti-CD44 (IM7; BioLegend), or anti–L-selectin mAb (MEL-14) for 10 min. In some experiments, cells were incubated with a mixture of 33 µg/ml (10 µg each mAb/mouse) MEL-14, 4RA10, and IM7 for 10 min. Equal numbers of CMTMR- and CFSE-labeled T cells were then mixed, and 300 µl of the lymphocyte suspension was injected intravenously (1.5×10^6 lymphocytes/mouse) into WT mice. After 2 h, lymphocyte suspensions of recipient lymphoid organs were analyzed by flow cytometry as described earlier in this section.

Flow cytometric analysis. Single-cell suspensions were prepared from NALT, PLNs, and spleens. The cell suspension was passed through a nylon mesh and incubated with various combinations of mAbs as follows: (1) APC-conjugated anti–mouse CD3ε (2C11; eBioscience), R-PE–conjugated anti–mouse CD19 (1D3; BD), APC-Cy7–conjugated anti–mouse CD4 (GK1.5; BioLegend), PE-Cy7–conjugated anti–mouse CD8 (53–6.7; BioLegend), and FITC-conjugated anti–mouse CD25 (7D4; Beckman Coulter) for differential staining of T and B cell subpopulations; (2) PE-conjugated anti–mouse CD4 (GK1.5; Beckman Coulter), FITC-conjugated anti–mouse CD25, and APC-conjugated anti–mouse CD62L (MEL-14; Beckman Coulter) for staining of L-selectin; and (3) biotin-conjugated anti–mouse CD3ε (2C11; BD), PE-conjugated anti–mouse CD4, APC-conjugated anti–mouse CD25 (PC61.5; eBioscience), and FITC-conjugated anti–mouse/human CD44 (IM7; BioLegend), followed by streptavidin-conjugated PerCP-Cy5.5 (BioLegend) for CD44 staining. For intracellular Foxp3 staining, cells were stained with a mouse T_{reg} cell staining kit (eBioscience) containing FITC-conjugated anti–mouse CD4 (RM4-5), APC-conjugated anti–mouse CD25 (PC61.5), and PE-conjugated anti–mouse/rat Foxp3 (FJK-16s) according to the manufacturer's instructions. The cells were analyzed by flow cytometry on a FACSCanto II (BD). The data were acquired and analyzed with FACS Diva software (BD) and FlowJo software (Tree Star, Inc.).

Purification of T_{reg} cells by FACS sorting. Lymphocytes from WT PLNs were stained with FITC-conjugated anti–mouse CD4 (RM4-5; eBioscience) and APC-conjugated anti–mouse CD25 (PC61.5; eBioscience) in PBS containing 0.1% BSA. After 30 min of incubation at 4°C, cells were washed, resuspended in PBS containing 2% FBS, and filtered through a cell strainer with a pore size of 40 µm (BD). $CD4^+CD25^+$ T_{reg} and $CD4^+CD25^-$ T_{conv} cells were sorted by a FACSAria II (BD), immersed in RNALater solution (Ambion), and stored at −80°C until use for real-time quantitative PCR. A portion of the sorted cells were stained with PE-conjugated anti–mouse/rat Foxp3 (FJK-16s; eBioscience) and analyzed on a FACSCanto II as described in the previous section.

Real-time quantitative PCR. Total RNA was extracted from the whole NALT, $CD4^+CD25^+$ T_{reg} cells, and $CD4^+CD25^-$ T_{conv} cells using the RNAspin Mini (GE Healthcare). cDNA was synthesized using PrimeScript RT-PCR kit (Takara Bio Inc.) and subjected to real-time quantitative PCR using SYBR Premix Ex Taq II (Takara Bio Inc.). The expression of each mRNA was normalized to the expression of β-actin with the ΔΔCt method according to the manufacturer's instructions (Thermal Cycler Dice TP870; Takara Bio Inc.). The primer sets used were as follows: β-actin, 5′-CATCCGTAAAGACCTCTATGCCAAC-3′ and 5′-ATGGAGCCACCGATCCACA-3′; IL-4, 5′-TCTCGAATGTACCAGGAGCCATATC-3′ and 5′-AGCACCTTGGAAGCCCTACAGA-3′; IL-10, 5′-ACCTGGTAGAAGTGATGCCCCAGGCA-3′ and 5′-CTATGCAGTTGATGAAGATGTCAAA-3′; TGF-β, 5′-GCAACATGTGGAACTCTACCAGAA-3′

and 5′-GACGTCAAAAGACAGCCACTCA-3′; Foxp3, 5′-CCCAGGAAAGACAGCAACCTT-3′ and 5′-TTCTCACAACCAGGCCACTTG-3′; FucT-VII, 5′-CTGAGAAGTTCTGGCGCAATG-3′ and 5′-TGACGAGGAAGACAGCCAGTT-3′; and PSGL-1, 5′-CTTCCTTGTGCTGCTGACCAT-3′ and 5′-TCAGGGTCCTCAAAATCGTCATC-3′.

Purification of HEV cells from NALT and RT-PCR. Freshly isolated NALT from 10 WT mice was minced with glass slides and suspended in ice-cold DME containing 10% FBS, 10 mM HEPES, 1 mg/ml collagenase A (Roche), 0.5 mg/ml dispase (Invitrogen), and 20 U/ml DNase I (Roche). The cell suspension was incubated for 60 min at 37°C with gentle shaking. After centrifugation, cells were resuspended in PBS containing 0.02% trypsin (Invitrogen) and 1 mM EDTA and incubated for 5 min at 37°C. DME containing 10% FBS and 10 mM HEPES was added to terminate the enzymatic digestion, and the cell suspension was passed through a 70-µm cell strainer (BD). The cells were incubated with 5 µg/ml biotin-conjugated mAb S2 (Hirakawa et al., 2010) for 10 min, washed with PBS containing 0.2% BSA, and incubated for 10 min with streptavidin-microbeads (1:10 dilution; Miltenyi Biotec). After washing, the cells were purified using the MS column in the Mini MACS according to the manufacturer's protocol (Miltenyi Biotec). The total RNA was purified from the mAb $S2^+$ cells (NALT HEV cells) and $CD4^+CD25^-$ T_{conv} cells, and used for RT-PCR. The primers used were: GlcNAc6ST-2, 5′-TCCATACTAACGCCAGGAACG-3′ and 5′-TGGTGACTAAGGCTGGAACC-3′; P-selectin, 5′-GCTTCAGGACAATGGACAGC-3′ and 5′-CTTTCTTAGCAGAGCCAGGAGTG-3′; and β-actin, 5′-TGGAATCCTGTGGCATCCATGAAAC-3′ and 5′-TAAAACGCAGCTCAGTAACAGTCCG-3′. The PCR cycle (94°C, 30 s; 62°C 30 s; 72°C 30 s) was repeated 42 times for GlcNAc6ST-2. The PCR cycle (94°C, 30 s; 65°C 30 s; 72°C 30 s) was repeated 42 times for P-selectin and 38 times for β-actin.

Intranasal immunization. WT and DKO mice were lightly anesthetized with sodium pentobarbital (Nembutal; Abbott) and immunized intranasally (in the left nostril) on days 0, 7, and 14 with 100 µg of OVA (Sigma-Aldrich) in PBS together with 1 µg cholera toxin (CT; EMD or List Biological Laboratories Inc.; used as a mucosal adjuvant) in a total volume of 12.5 µl per mouse. Control mice were given PBS in the same volume on days 0, 7, and 14. On day 21, serum and nasal wash (obtained by washing the nasal cavities with 10 µl PBS/nostril) were collected from each mouse and stored at −80°C until use for measurement of OVA-specific Abs. To assess nasal symptoms after intranasal immunization, mice were immunized on days 0, 7, 14, and 21 as described. 2 min after intranasal immunization on day 21, the number of sneezes in 5 min was counted. In separate experiments, mice were immunized on days 0, 7, and 14 as described, and the left NALT was collected on day 15, immersed in RNALater Solution, and stored at −80°C until use for real-time quantitative PCR.

Measurement of OVA-specific Abs. To detect OVA-specific IgE, the wells of a 96-well ELISA plate were first coated with 2 µg/ml anti–mouse IgE (BioLegend). After blocking, serially diluted serum was added to the well and incubated for 1 h. After washing, 2 µg/ml biotinylated OVA labeled with EZ-Link Sulfo-NHS-LC biotin (Thermo Fisher Scientific) was added and incubated for 1 h. After washing, 5 µg/ml peroxidase-conjugated streptavidin (Vector Laboratories) was added and incubated for 1 h. To detect OVA-specific IgG and IgA, the wells were first coated with unlabeled OVA. After blocking, serially diluted serum and nasal wash for the detection of IgG and IgA, respectively, were added to the wells and incubated for 1 h. After washing, peroxidase-conjugated goat anti–mouse IgG (1:3,000 dilution; Invitrogen) or anti–mouse IgA (1:1,000 dilution; Invitrogen) was added to the wells and incubated for 1 h. Finally, the HRP substrate 2,2′-azido-bis (3-ethylbenzothazoline-6-sulfonic acid) diammonium salt (ABTS; Wako Chemicals USA) was added, and the optical density at 405 nm was measured using a 96-well spectrometer (Spectra Rainbow Thermo; TECAN).

Statistical analysis. A student's *t* test was used for statistical analysis.

Online supplemental material. Fig. S1 shows expression of CCL21 and CXCL12 in NALT and PLNs in WT and DKO mice. Fig. S2 shows that anti–L-selectin mAb reduced OVA-specific IgE production and attenuated nasal symptoms. Fig. S3 shows expression of HA in NALT HEVs in WT and DKO mice. Fig. S4 shows expression of MECA-367 antigens in NALT HEVs in BALB/c mice. Fig. S5 shows that GlcNAc-6-*O*-sulfated glycans were eliminated from the NALT and PLN HEVs of DKO mice. Fig. S6 shows a proposed model for the molecular mechanisms of T_{reg} and T_{conv} cell homing to NALT and the reduction of allergic responses in DKO mice. Online supplemental material is available at http://www.jem.org/cgi/content/full/jem.20101786/DC1.

This work was supported in part by Grant-in-Aid for Scientific Research (B), Grant-in-Aid for Challenging Exploratory Research, and Grant-in-Aid for Scientific Research on Priority Areas, Dynamics of Extracellular Environments, from the Ministry of Education, Culture, Sports, Science and Technology, Japan (21390023, 22659018, and 20057022, respectively, to H. Kawashima), a Research Grant from the Takeda Science Foundation (to H. Kawashima), a Research Fellowship from the Japan Society for the Promotion of Science (to J. Hirakawa), and National Institutes of Health grant PO1CA71932 (to M. Fukuda).

The authors declare that they have no competing financial interests.

Submitted: 27 August 2010
Accepted: 22 March 2011

REFERENCES

Alon, R., D.A. Hammer, and T.A. Springer. 1995. Lifetime of the P-selectin-carbohydrate bond and its response to tensile force in hydrodynamic flow. *Nature*. 374:539–542. doi:10.1038/374539a0

Aruffo, A., I. Stamenkovic, M. Melnick, C.B. Underhill, and B. Seed. 1990. CD44 is the principal cell surface receptor for hyaluronate. *Cell*. 61:1303–1313. doi:10.1016/0092-8674(90)90694-A

Atarashi, K., T. Tanoue, T. Shima, A. Imaoka, T. Kuwahara, Y. Momose, G. Cheng, S. Yamasaki, T. Saito, Y. Ohba, et al. 2011. Induction of colonic regulatory T cells by indigenous *Clostridium* species. *Science*. 331:337–341. doi:10.1126/science.1198469

Berlin, C., E.L. Berg, M.J. Briskin, D.P. Andrew, P.J. Kilshaw, B. Holzmann, I.L. Weissman, A. Hamann, and E.C. Butcher. 1993. α 4 β 7 integrin mediates lymphocyte binding to the mucosal vascular addressin MAdCAM-1. *Cell*. 74:185–195. doi:10.1016/0092-8674(93)90305-A

Bosse, R., and D. Vestweber. 1994. Only simultaneous blocking of the L- and P-selectin completely inhibits neutrophil migration into mouse peritoneum. *Eur. J. Immunol.* 24:3019–3024. doi:10.1002/eji.1830241215

Butcher, E.C., and L.J. Picker. 1996. Lymphocyte homing and homeostasis. *Science*. 272:60–66. doi:10.1126/science.272.5258.60

Csencsits, K.L., M.A. Jutila, and D.W. Pascual. 1999. Nasal-associated lymphoid tissue: phenotypic and functional evidence for the primary role of peripheral node addressin in naive lymphocyte adhesion to high endothelial venules in a mucosal site. *J. Immunol.* 163:1382–1389.

Debertin, A.S., T. Tschernig, H. Tönjes, W.J. Kleemann, H.D. Tröger, and R. Pabst. 2003. Nasal-associated lymphoid tissue (NALT): frequency and localization in young children. *Clin. Exp. Immunol.* 134:503–507. doi:10.1111/j.1365-2249.2003.02311.x

DeGrendele, H.C., P. Estess, L.J. Picker, and M.H. Siegelman. 1996. CD44 and its ligand hyaluronate mediate rolling under physiologic flow: a novel lymphocyte-endothelial cell primary adhesion pathway. *J. Exp. Med.* 183:1119–1130. doi:10.1084/jem.183.3.1119

Foxall, C., S.R. Watson, D. Dowbenko, C. Fennie, L.A. Lasky, M. Kiso, A. Hasegawa, D. Asa, and B.K. Brandley. 1992. The three members of the selectin receptor family recognize a common carbohydrate epitope, the sialyl Lewis^x oligosaccharide. *J. Cell Biol.* 117:895–902. doi:10.1083/jcb.117.4.895

Frenette, P.S., C.V. Denis, L. Weiss, K. Jurk, S. Subbarao, B. Kehrel, J.H. Hartwig, D. Vestweber, and D.D. Wagner. 2000. P-Selectin glycoprotein ligand 1 (PSGL-1) is expressed on platelets and can mediate platelet–endothelial interactions in vivo. *J. Exp. Med.* 191:1413–1422. doi:10.1084/jem.191.8.1413

Gallatin, W.M., I.L. Weissman, and E.C. Butcher. 1983. A cell-surface molecule involved in organ-specific homing of lymphocytes. *Nature*. 304:30–34. doi:10.1038/304030a0

Gauguet, J.M., S.D. Rosen, J.D. Marth, and U.H. von Andrian. 2004. Core 2 branching β1,6-*N*-acetylglucosaminyltransferase and high endothelial cell N-acetylglucosamine-6-sulfotransferase exert differential control over B- and T-lymphocyte homing to peripheral lymph nodes. *Blood*. 104:4104–4112. doi:10.1182/blood-2004-05-1986

Gelfand, E.W. 2004. Inflammatory mediators in allergic rhinitis. *J. Allergy Clin. Immunol.* 114:S135–S138. doi:10.1016/j.jaci.2004.08.043

Girard, J.P., and T.A. Springer. 1995. High endothelial venules (HEVs): specialized endothelium for lymphocyte migration. *Immunol. Today.* 16:449–457. doi:10.1016/0167-5699(95)80023-9

Hellings, P., M. Jorissen, and J.L. Ceuppens. 2000. The Waldeyer's ring. *Acta Otorhinolaryngol. Belg.* 54:237–241.

Hirakawa, J., K. Tsuboi, K. Sato, M. Kobayashi, S. Watanabe, A. Takakura, Y. Imai, Y. Ito, M. Fukuda, and H. Kawashima. 2010. Novel anti-carbohydrate antibodies reveal the cooperative function of sulfated *N*- and *O*-glycans in lymphocyte homing. *J. Biol. Chem.* 285:40864–40878. doi:10.1074/jbc.M110.167296

Hiraoka, N., H. Kawashima, B. Petryniak, J. Nakayama, J. Mitoma, J.D. Marth, J.B. Lowe, and M. Fukuda. 2004. Core 2 branching β1,6-*N*-acetylglucosaminyltransferase and high endothelial venule-restricted sulfotransferase collaboratively control lymphocyte homing. *J. Biol. Chem.* 279:3058–3067. doi:10.1074/jbc.M311150200

Homeister, J.W., A.D. Thall, B. Petryniak, P. Malý, C.E. Rogers, P.L. Smith, R.J. Kelly, K.M. Gersten, S.W. Askari, G. Cheng, et al. 2001. The α(1,3)fucosyltransferases FucT-IV and FucT-VII exert collaborative control over selectin-dependent leukocyte recruitment and lymphocyte homing. *Immunity.* 15:115–126. doi:10.1016/S1074-7613(01)00166-2

Hori, S., T. Nomura, and S. Sakaguchi. 2003. Control of regulatory T cell development by the transcription factor Foxp3. *Science.* 299:1057–1061. doi:10.1126/science.1079490

Huehn, J., and A. Hamann. 2005. Homing to suppress: address codes for Treg migration. *Trends Immunol.* 26:632–636. doi:10.1016/j.it.2005.10.001

Imai, Y., T. Ishikawa, T. Tanikawa, H. Nakagami, T. Maekawa, and K. Kurohane. 2005. Production of IgA monoclonal antibody against Shiga toxin binding subunits employing nasal-associated lymphoid tissue. *J. Immunol. Methods.* 302:125–135. doi:10.1016/j.jim.2005.05.007

Imaoka, K., C.J. Miller, M. Kubota, M.B. McChesney, B. Lohman, M. Yamamoto, K. Fujihashi, K. Someya, M. Honda, J.R. McGhee, and H. Kiyono. 1998. Nasal immunization of nonhuman primates with simian immunodeficiency virus p55gag and cholera toxin adjuvant induces Th1/Th2 help for virus-specific immune responses in reproductive tissues. *J. Immunol.* 161:5952–5958.

Kawashima, H. 2006. Roles of sulfated glycans in lymphocyte homing. *Biol. Pharm. Bull.* 29:2343–2349. doi:10.1248/bpb.29.2343

Kawashima, H., B. Petryniak, N. Hiraoka, J. Mitoma, V. Huckaby, J. Nakayama, K. Uchimura, K. Kadomatsu, T. Muramatsu, J.B. Lowe, and M. Fukuda. 2005. *N*-acetylglucosamine-6-*O*-sulfotransferases 1 and 2 cooperatively control lymphocyte homing through L-selectin ligand biosynthesis in high endothelial venules. *Nat. Immunol.* 6:1096–1104. doi:10.1038/ni1259

Kiyono, H., and S. Fukuyama. 2004. NALT- versus Peyer's-patch-mediated mucosal immunity. *Nat. Rev. Immunol.* 4:699–710. doi:10.1038/nri1439

Kurono, Y., M. Yamamoto, K. Fujihashi, S. Kodama, M. Suzuki, G. Mogi, J.R. McGhee, and H. Kiyono. 1999. Nasal immunization induces Haemophilus influenzae-specific Th1 and Th2 responses with mucosal IgA and systemic IgG antibodies for protective immunity. *J. Infect. Dis.* 180:122–132. doi:10.1086/314827

Link, A., T.K. Vogt, S. Favre, M.R. Britschgi, H. Acha-Orbea, B. Hinz, J.G. Cyster, and S.A. Luther. 2007. Fibroblastic reticular cells in lymph nodes regulate the homeostasis of naive T cells. *Nat. Immunol.* 8:1255–1265. doi:10.1038/ni1513

Luther, S.A., H.L. Tang, P.L. Hyman, A.G. Farr, and J.G. Cyster. 2000. Coexpression of the chemokines ELC and SLC by T zone stromal cells and deletion of the ELC gene in the *plt/plt* mouse. *Proc. Natl. Acad. Sci. USA.* 97:12694–12699. doi:10.1073/pnas.97.23.12694

Mitoma, J., X. Bao, B. Petryanik, P. Schaerli, J.M. Gauguet, S.Y. Yu, H. Kawashima, H. Saito, K. Ohtsubo, J.D. Marth, et al. 2007. Critical functions of *N*-glycans in L-selectin-mediated lymphocyte homing and recruitment. *Nat. Immunol.* 8:409–418. doi:10.1038/ni1442

Moore, K.L., K.D. Patel, R.E. Bruehl, F. Li, D.A. Johnson, H.S. Lichenstein, R.D. Cummings, D.F. Bainton, and R.P. McEver. 1995. P-selectin glycoprotein ligand-1 mediates rolling of human neutrophils on P-selectin. *J. Cell Biol.* 128:661–671. doi:10.1083/jcb.128.4.661

Nakache, M., E.L. Berg, P.R. Streeter, and E.C. Butcher. 1989. The mucosal vascular addressin is a tissue-specific endothelial cell adhesion molecule for circulating lymphocytes. *Nature.* 337:179–181. doi:10.1038/337179a0

Nakano, H., and M.D. Gunn. 2001. Gene duplications at the chemokine locus on mouse chromosome 4: multiple strain-specific haplotypes and the deletion of secondary lymphoid-organ chemokine and EBI-1 ligand chemokine genes in the plt mutation. *J. Immunol.* 166:361–369.

Okada, T., V.N. Ngo, E.H. Ekland, R. Förster, M. Lipp, D.R. Littman, and J.G. Cyster. 2002. Chemokine requirements for B cell entry to lymph nodes and Peyer's patches. *J. Exp. Med.* 196:65–75. doi:10.1084/jem.20020201

Rosen, S.D. 2004. Ligands for L-selectin: homing, inflammation, and beyond. *Annu. Rev. Immunol.* 22:129–156. doi:10.1146/annurev.immunol.21.090501.080131

Rosen, S.D., M.S. Singer, T.A. Yednock, and L.M. Stoolman. 1985. Involvement of sialic acid on endothelial cells in organ-specific lymphocyte recirculation. *Science.* 228:1005–1007. doi:10.1126/science.4001928

Round, J.L., and S.K. Mazmanian. 2010. Inducible Foxp3$^+$ regulatory T-cell development by a commensal bacterium of the intestinal microbiota. *Proc. Natl. Acad. Sci. USA.* 107:12204–12209. doi:10.1073/pnas.0909122107

Sakaguchi, S. 2005. Naturally arising Foxp3-expressing CD25$^+$CD4$^+$ regulatory T cells in immunological tolerance to self and non-self. *Nat. Immunol.* 6:345–352. doi:10.1038/ni1178

Snapp, K.R., A.J. Wagers, R. Craig, L.M. Stoolman, and G.S. Kansas. 1997. P-selectin glycoprotein ligand-1 is essential for adhesion to P-selectin but not E-selectin in stably transfected hematopoietic cell lines. *Blood.* 89:896–901.

Springer, T.A. 1994. Traffic signals for lymphocyte recirculation and leukocyte emigration: the multistep paradigm. *Cell.* 76:301–314. doi:10.1016/0092-8674(94)90337-9

Streeter, P.R., B.T. Rouse, and E.C. Butcher. 1988. Immunohistologic and functional characterization of a vascular addressin involved in lymphocyte homing into peripheral lymph nodes. *J. Cell Biol.* 107:1853–1862. doi:10.1083/jcb.107.5.1853

Takamura, K., S. Fukuyama, T. Nagatake, D.Y. Kim, A. Kawamura, H. Kawauchi, and H. Kiyono. 2007. Regulatory role of lymphoid chemokine CCL19 and CCL21 in the control of allergic rhinitis. *J. Immunol.* 179:5897–5906.

Uchimura, K., H. Muramatsu, K. Kadomatsu, Q.W. Fan, N. Kurosawa, C. Mitsuoka, R. Kannagi, O. Habuchi, and T. Muramatsu. 1998. Molecular cloning and characterization of an *N*-acetylglucosamine-6-*O*-sulfotransferase. *J. Biol. Chem.* 273:22577–22583. doi:10.1074/jbc.273.35.22577

Uchimura, K., J.M. Gauguet, M.S. Singer, D. Tsay, R. Kannagi, T. Muramatsu, U.H. von Andrian, and S.D. Rosen. 2005. A major class of L-selectin ligands is eliminated in mice deficient in two sulfotransferases expressed in high endothelial venules. *Nat. Immunol.* 6:1105–1113. doi:10.1038/ni1258

Venturi, G.M., R.M. Conway, D.A. Steeber, and T.F. Tedder. 2007. CD25$^+$CD4$^+$ regulatory T cell migration requires L-selectin expression: L-selectin transcriptional regulation balances constitutive receptor turnover. *J. Immunol.* 178:291–300.

von Andrian, U.H., and T.R. Mempel. 2003. Homing and cellular traffic in lymph nodes. *Nat. Rev. Immunol.* 3:867–878. doi:10.1038/nri1222

Yeh, J.C., N. Hiraoka, B. Petryniak, J. Nakayama, L.G. Ellies, D. Rabuka, O. Hindsgaul, J.D. Marth, J.B. Lowe, and M. Fukuda. 2001. Novel sulfated lymphocyte homing receptors and their control by a Core1 extension β 1,3-*N*-acetylglucosaminyltransferase. *Cell.* 105:957–969. doi:10.1016/S0092-8674(01)00394-4

Yoshida, R., T. Imai, K. Hieshima, J. Kusuda, M. Baba, M. Kitaura, M. Nishimura, M. Kakizaki, H. Nomiyama, and O. Yoshie. 1997. Molecular cloning of a novel human CC chemokine EBI1-ligand chemokine that is a specific functional ligand for EBI1, CCR7. *J. Biol. Chem.* 272:13803–13809. doi:10.1074/jbc.272.21.13803

Yoshida, R., M. Nagira, M. Kitaura, N. Imagawa, T. Imai, and O. Yoshie. 1998. Secondary lymphoid-tissue chemokine is a functional ligand for the CC chemokine receptor CCR7. *J. Biol. Chem.* 273:7118–7122. doi:10.1074/jbc.273.12.7118

Zhang, N., B. Schröppel, G. Lal, C. Jakubzick, X. Mao, D. Chen, N. Yin, R. Jessberger, J.C. Ochando, Y. Ding, and J.S. Bromberg. 2009. Regulatory T cells sequentially migrate from inflamed tissues to draining lymph nodes to suppress the alloimmune response. *Immunity.* 30:458–469. doi:10.1016/j.immuni.2008.12.022

Zhu, J., and W.E. Paul. 2008. CD4 T cells: fates, functions, and faults. *Blood.* 112:1557–1569. doi:10.1182/blood-2008-05-078154